Available online at www.sciencedirect.com
ScienceDirect
Trans. Nonferrous Met. Soc. China 22(2012) 1918−1923
Transactions of Nonferrous Metals Society of China
www.tnmsc.cn

Dry sliding wear behavior of cast Mg−11Y−5Gd−2Zn magnesium alloy

HU Mao-liang[1, 2], WANG Qu-dong[1], LI Cheng[1], DING Wen-jiang[1]

1. National Engineering Research Center of Light Alloy Net Forming, Shanghai Jiao Tong University, Shanghai 200240, China;
2. School of Materials Science and Engineering, Harbin University of Science and Technology, Harbin 150040, China

Received 10 November 2011; accepted 31 May 2012

Abstract: Dry sliding wear tests on as-cast and cast+T6 Mg−11Y−5Gd−2Zn magnesium alloys were performed using a ball-on-plate configuration. The wear rates were measured within a load range of 3−15 N, sliding speed range of 0.03−0.24 m/s, test temperature range of 25−200 °C and at a constant sliding distance of 400 m. The wear tracks, worn surfaces and wear debris of the alloys were analyzed using scanning electron microscope (SEM). The results show that the wear rate of the alloys increases almost linearly with increasing applied load and decreases with increasing sliding speed. The wear rate of the as-cast alloy is higher than that of the cast+T6 alloy. The amount of $Mg_{12}Y_1Zn_1$ phase, surface oxidation and retained wear debris affect the wear rate. The dominant wear mechanisms under the test condition are abrasion and plastic deformation.

Key words: Mg−Y−Gd−Zn alloy; wear behavior; wear rate; sliding wear; abrasive wear

1 Introduction

Magnesium alloys as the lightest structural metal have attracted considerable interest from the automobile and aerospace industries where the lightweighting is becoming urgent [1,2]. However, the poor resistance to wear and corrosion is a serious impediment against the wider application of magnesium alloys, and prevent them from being used as widely as aluminium alloys [3,4]. In certain applications, magnesium alloys are submitted to unlubricated wear conditions and the failure of their products is usually caused by dynamic friction against foreign objects during service. The sliding wear behavior of magnesium alloys is an important consideration.

There are some works dealing on the wear behaviour of magnesium alloys such as Mg−Al−Zn [5,6], Mg−Zn−Y [3,7] and Mg−Zn−Ce [8,9]. AZ91D alloy shows lower wear rate than AS21 aluminium alloy against sintered iron alloy [5] and fluctuates with sliding speed leading to three different wear transitions [6]. Mg97Zn1Y2 alloy has a better tribological property than AZ91 alloy under high load [3]. Mg−25Zn−2Y quasicrystal alloy exhibits low friction coefficient and good wear resistance [7]. Dry sliding wear behaviour of ZE41A alloy has been is developed and classified using wear mechanism maps [8,9]. However, few studies have been carried out to understand the sliding wear behaviour of Mg−Gd−Y−Zn alloys.

Mg−Gd−Y−Zn alloys are particularly attractive because of their excellent mechanical properties [10−12]. The addition of rare earths to magnesium significantly improves its strength and creep resistance combined with good castability. Considerable researches have been carried out to study the mechanical property, corrosion resistance and fatigue behaviour of the Mg−Gd−Y alloys [10,13].

In the present work, dry sliding wear behaviour of a Mg−11Y−5Gd−2Zn magnesium alloy in the as-cast and cast+T6 heat treated conditions is investigated using a ball-on-plate configuration. The effect of applied load, sliding speed and test temperature on the wear phenomena is thoroughly studied.

2 Experimental

The Mg−11Y−5Gd−2Zn alloy was prepared from high purity Mg (99.95%), Zn (99.99%), Mg−25%Gd and

Foundation item: Project (51074106) supported by the National Natural Science Foundation of China; Project (2009AA033501) supported by the Hi-Tech Research and Development Program of China; Project (09JC1408200) supported by the Science and Technology Commission of Shanghai Municipality, China; Project (20100480586) supported by Postdoctoral Science Foundation of China
Corresponding author: WANG Qu-dong; Tel: +86-21-54742715; E-mail: wangqudong@sjtu.edu.cn
DOI: 10.1016/S1003-6326(11)61408-8

Mg−25%Y (mass fraction) master alloys in an electric resistance furnace under a mixed flowing protective gas of CO_2 and SF_6 with a volume ratio of 100:1. The actual composition of the cast ingot is listed in Table 1, measured using an inductively coupled plasma (ICP) analyzer. The as-cast alloy was solution heat treated at 535 °C for 20 h and quenched into 60 °C water. T6 peak-aging heat treatment involved aging in a hot oil bath at 225 °C for 24 h followed by air cooling. The density of the cast+T6 alloy was 1.995 g/cm^3, and the Vickers hardness of cast+T6 alloy was HV136 under a load of 49 N for holding time of 15 s.

Table 1 Composition of Mg−11Y−5Gd−2Zn alloys (mass fraction, %)

Alloy	Composition/%			
	Y	Gd	Zn	Mg
Normal	11	5	2	Bal.
Actual	11.52	5.21	1.75	Bal.

Dry sliding wear tests were performed using a ball-on-plate configuration. The counter-faces were AISI 52100 steel bearing balls of 6 mm in diameter with hardness of 61 on the Rockwell-C scale. Before the test, rectangular specimens with dimensions of 50 mm× 30 mm×5 mm were cut from the ingot by an electric-spark wire-cutting machine. The surface preparation procedure of the wear test samples consisted of grinding surfaces manually by 240, 400 and 800 grit SiC papers, sequentially and then polishing with 1.0 and 0.05 μm alumina powder slurry using a low-speed polishing machine. The polished surfaces were cleaned in an ultrasonic bath using alcohol before wear tests.

The wear tests were conducted in a load range of 3−15 N and a velocity range of 0.03−0.24 m/s corresponding to a temperature range of 25−200 °C for a constant sliding distance of 400 m. The stroke length was 30 mm in the middle surface of the plate specimen.

The mass losses were calculated from the mass difference of specimens measured before and after the sliding tests after removing any loose debris from the worn surface. The volumetric wear loss was estimated by dividing the mass loss by the density of the alloy. The wear rate k was calculated using the following equation:

$$k=\frac{m}{\rho L}$$

where m is the mass loss; ρ is the density of magnesium alloy and L is the sliding distance. The worn surfaces and wear debris collected from the surface were examined using scanning electron microscope (SEM). Each test was carried out at least twice in order to check the reproducibility and the average value of the tests was taken to determine the wear rate.

3 Results and discussion

3.1 Initial microstructure

Figure 1 and Table 2 show the SEM images of the as-cast and cast+T6 Mg−11Y−5Gd−2Zn alloy and the corresponding EDX analysis results, respectively. It is found that the as-cast alloy consists of α-Mg (Point A1 in Fig. 1(a)), eutectic phase $Mg_{24}(YGdZn)_5$ (Point B1 in Fig. 1(a)) and $Mg_{12}Y_1Zn_1$ phase (Point C1 in Fig. 1(a)). $Mg_{24}(YGdZn)_5$ phase looks like narrow island morphology and is distributed randomly in the grain boundary. $Mg_{12}Y_1Zn_1$ phase presents needle-shaped and plate-shaped morphology and is distributed near the grain boundary. After solution treatment at 535 °C for 20 h and aging treatment at 225 °C for 24 h, some eutectic phase $Mg_{24}(YGdZn)_5$ is dissolved in the matrix and residual $Mg_{24}(YGdZn)_5$ (Point B2 in Fig. 1(b))

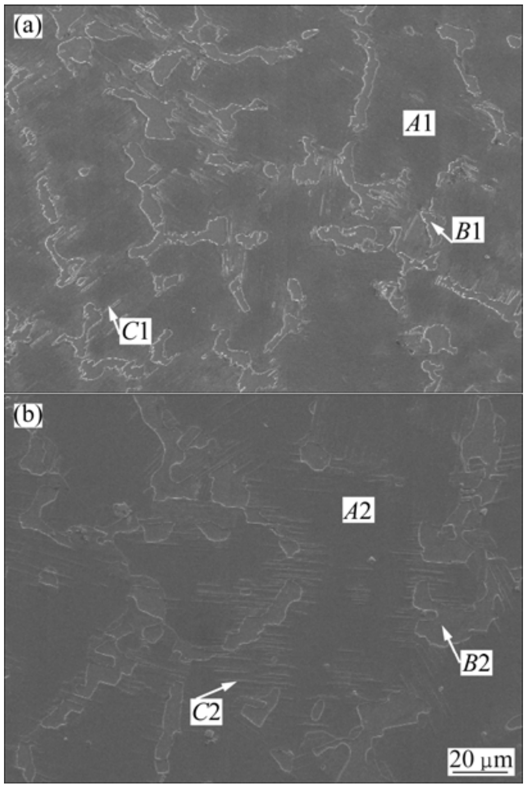

Fig. 1 SEM images of Mg−11Y−5Gd−2Zn plate specimens: (a) As-cast; (b) Cast+T6

Table 2 EDX analysis results of as-cast and cast+T6 Mg−11Y−5Gd−2Zn alloys in Fig. 1 (molar fraction, %)

Element	Point A1	Point B1	Point C1	Point A2	Point B2	Point C2
Mg	96.77	86.67	89.39	95.91	86.16	91.84
Y	2.33	10.01	7.33	2.93	10.13	4.98
Gd	0.57	2.34	0.05	0.70	2.13	0.07
Zn	0.33	0.98	3.23	0.46	1.58	3.11

becomes passivation. $Mg_{12}Y_1Zn_1$ phase (Point *C*2 in Fig. 1(b)) obviously increases and randomly distributes from the grain boundary to the inner of *α*-Mg. Further details regarding the precipitation behavior during solution treatment and aging treatment of Mg−11Y−5Gd−2Zn alloy using scanning electron microscopy and transmission electron microscopy are provided in previous studies [12,14].

3.2 Wear rate

The wear rates of the as-cast and cast+T6 Mg−11Y−5Gd−2Zn alloy are plotted against the applied load in Fig. 2. It is evident that the wear rate of the as-cast alloy is higher than that of the cast+T6 alloy under all applied loads. For example, the wear rate of the as-cast alloy is higher than that of the cast+T6 alloy by 37.3% under 7 N load. And the wear rates of the as-cast and cast+T6 Mg−11Y−5Gd−2Zn alloy increase almost linearly with the increase of applied load.

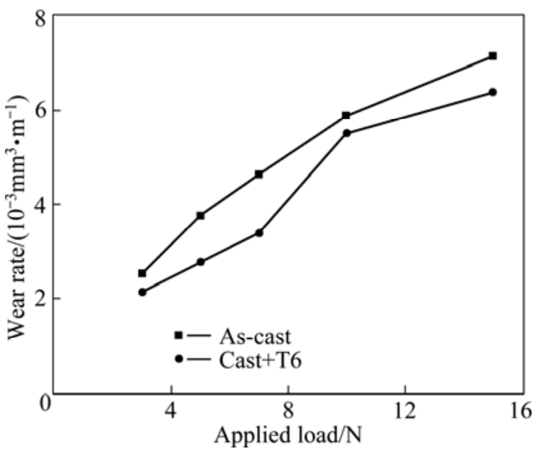

Fig. 2 Wear rate of as-cast and cast+T6 Mg−11Y−5Gd−2Zn alloys as function of applied load at sliding speed of 0.06 m/s and temperature of 25 °C for 400 m sliding distance

The wear rates of the as-cast and cast+T6 Mg−11Y−5Gd−2Zn alloys are plotted against the sliding speed in Fig. 3. The wear rate decreases with increasing sliding speed. In a sliding speed range of 0.03−0.12 m/s, the wear rate of as-cast alloy is higher than that of the cast+T6 alloy, and when the sliding speed exceeds 0.12 m/s, the wear rate of cast+T6 alloy slightly decreases and exceeds the value of as-cast alloy.

The wear rates of the as-cast and cast+T6 Mg−11Y−5Gd−2Zn alloys are plotted against the test temperature in Fig. 4. The wear rate of the as-cast alloy is higher than that of the cast+T6 alloy. For the as-cast alloy, the wear rate gradually decreases with increasing test temperature. The wear rate of cast+T6 alloy presents a maximum value during sliding at 373 K and it rapidly decreases with increasing test temperature from 373 to 473 K.

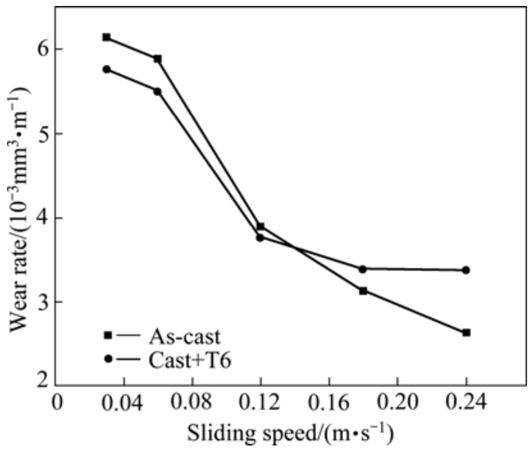

Fig. 3 Variation of wear rate with sliding speed for as-cast and cast+T6 Mg−11Y−5Gd−2Zn alloys under applied load of 10 N and temperature of 25 °C for 400 m sliding distance

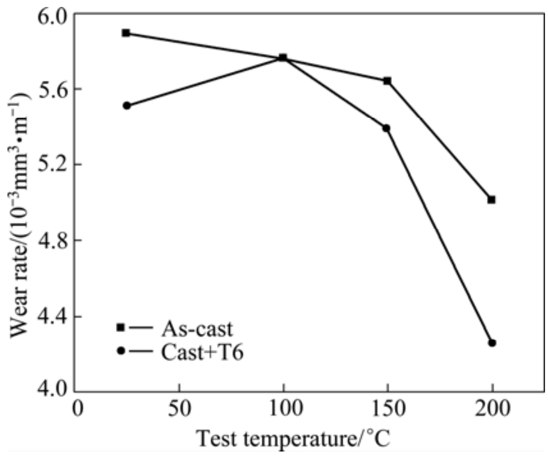

Fig. 4 Variation of wear rate with test temperature for as-cast and cast+T6 Mg−11Y−5Gd−2Zn alloys under normal load of 10 N and sliding speed of 0.06 m/s for 400 m sliding distance

For the cast+T6 Mg−11Y−5Gd−2Zn alloy, the amount of $Mg_{12}Y_1Zn_1$ phase obviously increases and randomly distributes from the grain boundary to the inner of *α*-Mg. $Mg_{12}Y_1Zn_1$ phase has a higher strength and better thermal stability than *α*-Mg which is supersaturated with Y, Gd and Zn [14,15]. At the same time, $Mg_{12}Y_1Zn_1$ phase can effectively pin the grain boundary sliding [16,17]. $Mg_{12}Y_1Zn_1$ phase can act as a second hard phase and resist the material flow during the wear process, so the wear rate of as-cast alloy is higher than that of cast+T6 alloy, as shown in Fig. 2.

With increasing sliding speed, the generated frictional heat gradually affects the wear rate of the alloy, as shown in Fig. 3. Higher relative motion results in higher contacting temperature between the alloy and the steel ball, which could oxidize the surface [9]. The surface oxidation has a protective effect against wear damage and decreases the wear rate. The results suggest that the effect of surface oxidation for the as-cast alloy is higher than that for the cast+T6 alloy, and the wear rate of the as-cast alloy is lower than that of the cast+T6 alloy at sliding speed of 0.18 and 0.24 m/s.

With increasing test temperature, the effect of surface oxidation on wear rate is similar to increasing the sliding speed. Higher test temperature is easy to oxidize the surface during the wear test and decreases the wear rate. On the other hand, with increasing test temperature, the effect of resisting the material flow of $Mg_{12}Y_1Zn_1$ phase decreases and the wear rate increases. The results suggest that $Mg_{12}Y_1Zn_1$ phase plays an important role in increasing the wear rate at test temperature of 100 °C. So, the wear rate of the cast+T6 alloy presents a maximum value during sliding at 100 °C, as shown in Fig. 4.

3.3 Worn surface

Figure 5 shows the worn surfaces of the cast+T6 Mg−11Y−5Gd−2Zn alloy. It reveals that the worn surfaces are covered with continuous grooves parallel to the sliding direction. These parallel grooves are proof of ploughing [18]. The ploughing is formed by the steel ball and severe plastic deformation of the alloy on the surface.

The dominant wear mechanisms under the test condition of the alloy are abrasion and plastic deformation. Under low load (3 N, as shown in Fig. 5(a)),

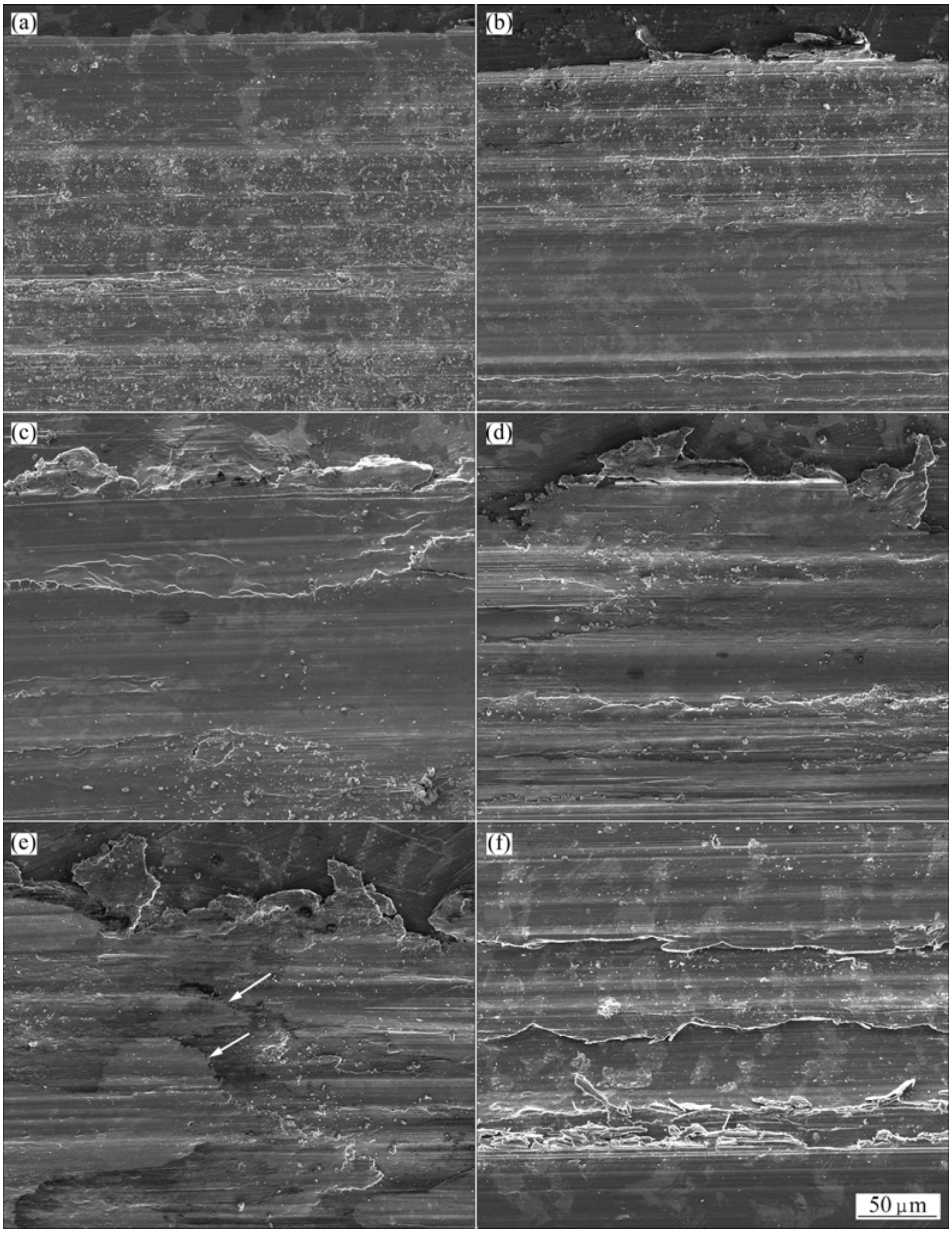

Fig. 5 SEM images of worn surface for cast+T6 Mg−11Y−5Gd−2Zn alloy under different wear conditions: (a) 0.06 m/s, 3 N, 298 K; (b) 0.06 m/s, 10 N, 298 K; (c) 0.06 m/s, 15 N, 298 K; (d) 0.12 m/s, 10 N, 298 K; (e) 0.24 m/s, 10 N, 298 K; (f) 0.06 m/s, 10 N, 473 K

the ploughing forms shallow fine grooves. Under a relatively high load (10 and 15 N, as shown in Figs. 5(b) and (c)), the width and depth of the ploughing grooves increase with the increase of the applied load. Increasing applied load results in higher wear rate of the alloy, as shown in Fig. 2.

With increasing sliding speed (0.12 and 0.24 m/s, as shown in Figs. 5(d) and (e)), the testing machine runs unstably, making a shrill sound. The straight grooves at a sliding speed of 0.24 m/s become wavy as marked by white arrows in Fig. 5(e). The wavy grooves result from the severe adhesion between friction pair. At the same time, a severely deformed material layer is flowed out of the contact surface perpendicular to the sliding direction. The layer is 30−60 μm in width and easy to be detached from the alloy. Worn surface at a high test temperature of 473 K is also covered with continuous grooves, and the width of the grooves increases, as shown in Fig. 5(f).

3.4 Wear debris

Figure 6 shows the wear debris morphologies of the cast+T6 Mg−11Y−5Gd−2Zn alloy collected after the wear tests. Under low load (3 N, as shown in Fig. 6(a)), the abrasive wear process results in the loss of fine debris particles, and these particles are less than 10 μm. With increasing applied load (15 N, as shown in Fig. 6(b)), these particles increase in length and thickness. This tendency agrees well with the wear rate.

With increasing sliding speed to 0.24 m/s, as shown in Fig. 6(c), some large round flakes appear and the diameter reaches 120 μm. At higher sliding speed, the wear debris is not easy to remove from the mating surface because the testing machine runs unstably. Plenty of wear debris is retained in the wear system and recycled in the mating surface, and large flakes form. This is another reason for the lower wear rate with increasing sliding speed. These large flakes are easy to fragment.

With increasing test temperature, as shown in Fig. 6(d), the wear debris changes to the slight dark colour particles. A colour difference between grey and black debris may be caused by a deficiency in Mg or O atoms within the MgO lattice [6]. At higher test temperature, an increasing heat facilitates the formation of oxidized areas over the worn surface. The oxidized metal debris assists in compaction of the debris to give the wear protective layer, and the layer results in effective protection against wear damage. It is difficult to establish the abrasive between fresh alloy and the hardened steel counter-face. So the wear rate decreases with increasing test temperature.

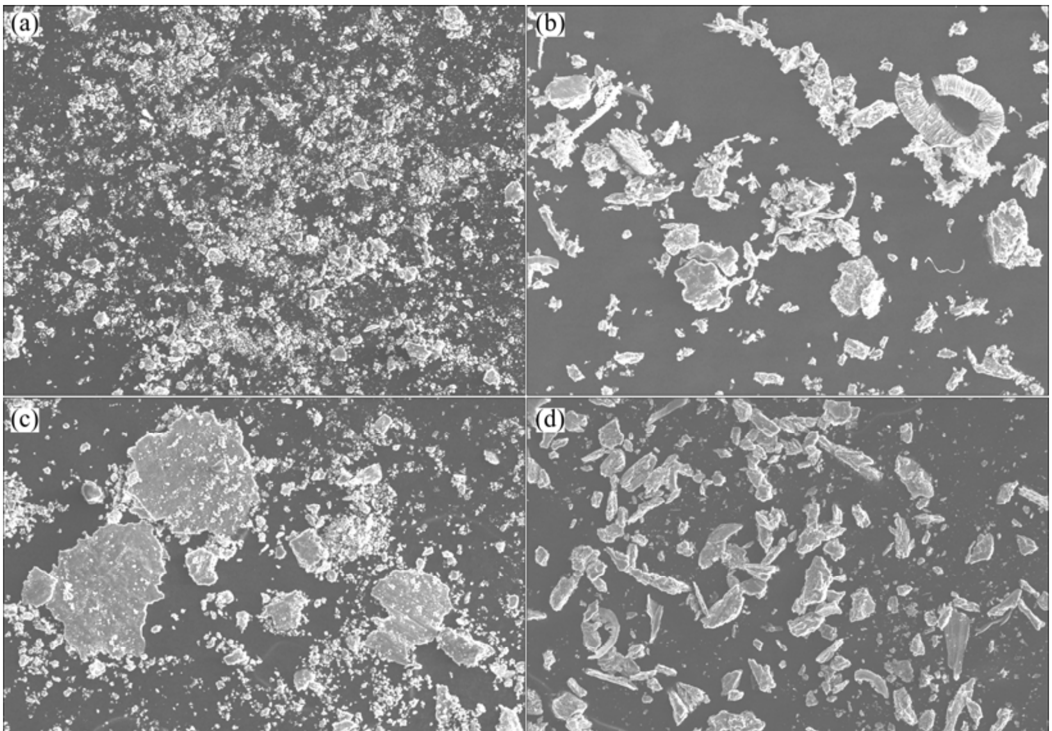

Fig. 6 SEM images of debris for cast+T6 Mg−11Y−5Gd−2Zn alloy under different wear conditions: (a) 0.06 m/s, 3 N, 298 K; (b) 0.06 m/s, 15 N, 298 K; (c) 0.24 m/s, 10 N, 298 K; (d) 0.06 m/s, 10 N, 473 K

4 Conclusions

1) The wear rates of the as-cast and cast+T6 Mg−11Y−5Gd−2Zn alloys increase almost linearly with increasing applied load and decrease with increasing sliding speed in an applied load range of 3−15 N and sliding speed range of 0.03−0.24 m/s at a constant sliding distance of 400 m.

2) For the Mg−11Y−5Gd−2Zn alloy, more $Mg_{12}Y_1Zn_1$ phase obviously reduces the wear rate, and the wear rate of the as-cast Mg−11Y−5Gd−2Zn alloy is higher than that of the cast+T6 Mg−11Y−5Gd−2Zn alloy.

3) Under higher test temperature conditions for the Mg−11Y−5Gd−2Zn alloy, the surface oxidation, $Mg_{12}Y_1Zn_1$ phase and retained wear debris reduce the wear rate.

4) Abrasion and plastic deformation are considered to be the dominant wear mechanisms for the Mg−11Y−5Gd−2Zn alloy.

References

[1] MORDIKE B L, EBERT T. Magnesium: properties— applications—potential [J]. Materials Science and Engineering A, 2001, 302(1): 37−45.

[2] CARPENTER J A, JACKMAN J, LI N Y, OSBORNE R J, POWELL B R, SKLAD P. Automotive Mg research and development in North America [J]. Materials Science Forum, 2007, 546−549: 11−24.

[3] AN J, LI R G, LU Y, CHEN C M, XU Y, CHEN X, WANG L M. Dry sliding wear behaviour of magnesium alloys [J]. Wear, 2008, 265(1−2): 97−104.

[4] GRAY J E, LUAN B. Protective coating on magnesium and its alloys—A critical review [J]. Journal of Alloys and Compounds, 2002, 336(1−2): 88−113.

[5] MEHTA D S, MASOOD S H, SONG W Q. Investigation of wear properties of magnesium and aluminium alloys for automotive applications [J]. Journal of Materials Processing Technology, 2004, 155−156: 1526−1531.

[6] AUNG N N, ZHOU W, LIM L E N. Wear behaviour of AZ91D alloy at low sliding speeds [J]. Wear, 2008, 265(5−6): 780−786.

[7] ZHANG Ying-bo, YU Si-rong, LUO Yan-ru, HU Hai-xia. Friction and wear behaviour of as-cast Mg−Zn−Y quasicrystal materials [J]. Materials Science and Engineering A, 2008, 472(1−2): 59−65.

[8] LOPEZ A J, RODRIGO P, TORRES B, RAMS J. Dry sliding wear behaviour of ZE41A magnesium alloy [J]. Wear, 2011, 271(11−12): 2836−2844.

[9] ANBUSELVAN S, RAMANATHAN. A comparative study of the wear behaviour of as-cast and hot extruded ZE41A magnesium alloy [J]. Journal of Alloys and Compounds, 2010, 502(2): 495−502.

[10] SUN Ming, WU Guo-hua, WANG Wei, DING Wen-jiang. Effect of Zr on the microstructure, mechanical properties and corrosion resistance of Mg−10Gd−3Y magnesium alloy [J]. Materials Science and Engineering A, 2009, 523(1−2): 145−151.

[11] GAO Yan, WANG Qu-dong, GU Jin-hai, ZHAO Yang, TONG Yan, KANEDA J. Effects of heat treatments on microstructure and mechanical properties of Mg−15Gd−5Y−0.5Zr alloy [J]. Journal of Rare Earths, 2008, 26(2): 298−302.

[12] YIN D D, WANG Q D, GAO Y, CHEN C J, ZHENG J. Effects of heat treatments on microstructure and mechanical properties of Mg−11Y−5Gd−2Zn−0.5Zr (wt.%) alloy [J]. Journal of Alloys and Compounds, 2011, 509(5): 1696−1704.

[13] CHANG Jian-wei, GUO Xing-wu, HE Shang-ming, FU Peng-huai, PENG Li-ming, DING Wen-jiang. Investigation of the corrosion for Mg−*x*Gd−3Y−0.4Zr (*x*=6, 8, 10, 12wt%) alloys in a peaked-aged condition [J]. Corrosion Science, 2008, 50(1): 166−177.

[14] CHEN C J, WANG Q D, YIN D D. Thermal properties of Mg−11Y−5Gd−2Zn−0.5Zr (wt.%) alloy [J]. Journal of Alloys and Compounds, 2009, 487(1−2): 560−563.

[15] LIN Dan, WANG Lei, MENG Fan-qiang, CUI Jian-zhong, LE Qi-chi. Effects of second phases on fracture behavior of Mg–10Gd–3Y–0.6Zr alloy [J]. Transactions of Nonferrous Metals Society of China, 2010, 20(s2): s421−s425.

[16] MATSUDA M, LI S, KAWAMURA Y, IKUHARA Y, NISHIDA M. Interaction between long period stacking order phase and deformation twin in rapidly solidified $Mg_{97}Zn_1Y_2$ alloy [J]. Materials Science and Engineering A, 2004, 386(1−2): 447−452.

[17] WANG Qu-dong, GAO Yan, YIN Dong-di, CHEN Chang-jiang. Characterization of phases in Mg–10Y–5Gd–2Zn–0.5Zr alloy [J]. Transactions of Nonferrous Metals Society of China, 2010, 20(11): 2076–2080.

[18] MONDAL A K, KUMAR S. Dry sliding wear behavior of magnesium alloy based hybrid composites in the longitudinal direction [J]. Wear, 2009, 267(1−4): 458−466.

Mg−11Y−5Gd−2Zn 镁合金干滑动的摩擦磨损行为

胡茂良 [1,2]，王渠东 [1]，李 程 [1]，丁文江 [1]

1. 上海交通大学 轻合金精密成型国家工程研究中心，上海 200240；

2. 哈尔滨理工大学 材料科学与工程学院，哈尔滨 150040

摘 要：采用往复式摩擦磨损试验机对铸态和 T6 态 Mg−11Y−5Gd−2Zn 合金进行干摩擦磨损试验，研究载荷(3~15 N)、磨擦速度(0.03~0.24 m/s)、摩擦温度(25~200 °C)对合金磨损率的影响，并通过扫描电镜观察合金磨损表面形貌和磨屑。结果表明：随着载荷的增加，合金的磨损率几乎呈线性增加；随着摩擦速率的增加，合金的磨损率降低；铸态合金的磨损率高于 T6 态合金的。Mg−11Y−5Gd−2Zn 合金中的 $Mg_{12}Y_1Zn_1$ 相、表面氧化相和残留的磨屑影响合金的磨损率。在本试验条件下，磨损机制主要是粘着磨损和塑性变形。

关键词：Mg−Y−Gd−Zn 合金；摩擦磨损行为；磨损率；滑动磨损；粘着磨损

(Edited by FANG Jing-hua)